

## Testing the daytime oxidizing capacity of the troposphere: 1994 OH field campaign at the Izaña observatory, Tenerife

W.Armerding, F.J.Comes, H.J.Crawack, O.Forberich, G.Gold, C. Ruger, M.Spiekermann,  
and J.Walter

Institut für Physikalische und Theoretische Chemie der J. W. Goethe Universität, Frankfurt, Germany

E. Cuevas and A. Redondas

Izaña GAW Station, Instituto Nacional de Meteorología, Santa Cruz de Tenerife  
Islas Canarias, Spain

R. Schmitt and P. Matuska

Meteorologie Consult, Glashütten, Germany

**Abstract.** A field campaign was carried out during May 1994 at the Izaña station, Tenerife. This campaign was part of the program Environment and Climate sponsored by the European Commission to study the influence of European emissions on the oxidizing capacity of a clean tropospheric environment. Daytime and also nighttime measurements were made, covering the OH as well as the NO<sub>3</sub> chemistry. This paper presents the OH measurements taken with a multipass optical absorption spectrometer (MOAS) and discusses the daytime chemistry in a statistical and therefore more preliminary way. All relevant parameters influencing the OH concentration were monitored. From the data the two main contributions to the OH production can clearly be discerned and are given by the primary production following the ozone photolysis and the O(<sup>1</sup>D)-H<sub>2</sub>O reaction and by the catalytic reactions of NO<sub>x</sub> in the recycling process. The latter processes prove to contribute a dominant part to the OH concentration. The measurements of the nonmethane hydrocarbons (NMHC) especially of the biogenics, indicate a considerable influence of the NMHC on the absolute values of the OH concentration at Tenerife.

### 1. Introduction

Three components are generally responsible for the oxidizing capacity of the troposphere: hydroxyl (OH), nitrate (NO<sub>3</sub>), and ozone (O<sub>3</sub>) [Finlayson-Pitts and Pitts, 1986a]. Being radicals, hydroxyl and nitrate are chemically unstable because of their high chemical reactivity. They are rather short-lived whereas ozone is a more "stable" compound, having a much longer lifetime in ambient air so that it is present at day and night. Both radicals, however, are formed from ozone, in which case ozone is either a precursor molecule or a reactant. The radiation of the sun which penetrates into the troposphere photolyzes the ozone at its short wavelength limit in the ultraviolet and forms metastable oxygen atoms in the <sup>1</sup>D state. These atoms react with the ubiquitous water vapor to directly produce the OH radicals. The hydroxyl radical therefore needs irradiation by sunlight to form in appreciable amounts, and it is mainly a daytime reactant. The nitrate radicals are, on the other hand, formed by a reaction of ozone with nitrogen dioxide. They only exist at significant concentrations during the night because they photolyze strongly

during day due to their high absorption [Finlayson-Pitts and Pitts, 1986b].

In an attempt to test the oxidizing capacity of the troposphere, we have carried out a campaign at the Izaña station, Tenerife. It is one of the sites selected for field measurements in the European program Environment and Climate, in which several European groups work together to investigate the impact of European emissions on a clean environment. The Izaña observatory is distinguished by its chemical, meteorological, and geographic conditions, and it provides in addition the infrastructure required for the ambitious field experiments. Tenerife represents in general a remote area with chemically aged air of Atlantic origin. Occasionally it is under the influence of younger air masses from the European and the African continent and from the United States where the impact of anthropogenic emissions can be seen.

The basic concept of the reported field campaign was to perform measurements of both the daytime and nighttime oxidizing efficiency of the troposphere, by monitoring the free radicals OH and NO<sub>3</sub> including the controlling parameters at a site with clean air, and to provide a database for model predictions comparable with measurements. The study of both radicals OH and NO<sub>3</sub> will enable us to obtain a nearly complete picture of the oxidizing capacity of the regional troposphere.

In particular, OH, as the main representative of the troposphere's daytime oxidizing capacity is very reactive and

Copyright 1997 by the American Geophysical Union.

Paper number 96JD03714.  
0148-0227/97/96JD-03714\$09.00

interacts chemically with many tropospheric trace gases. It drives the chemistry of both polluted and clean air. It initiates chain reactions by attack on organics and CO, and these chains are propagated through reactions with NO<sub>x</sub>. A simple balance between approximate production and consumption rates, with appropriate values of solar flux and concentrations of these controlling parameters, leads to a chemical lifetime for OH of about 1 s and maximum daytime concentrations on the 10<sup>6</sup> molecules cm<sup>-3</sup> level in the clean troposphere. Because of this short lifetime, the OH concentration responds rapidly to changes in the ambient concentrations of other atmospheric species, such as O<sub>3</sub>, H<sub>2</sub>O, NO [Ehhalt *et al.*, 1991; Comes, 1994].

The present paper is one of a series of three. It contains the results from the OH measurements obtained with the multipass optical absorption spectroscopy (MOAS) instrument and the necessary supplementary measurements. The OH measurements obtained during the campaign, nearly 1000 single OH determinations, have been correlated with the different parameters. They clearly show the influence of these parameters on the measured OH concentration at Tenerife. OH is found to be highly sensitive to the recycling mechanism due to the catalytic reactions of NO<sub>x</sub>. Also the determination of the ancillary data is discussed briefly.

The second paper discusses the results obtained with a differential optical absorption spectroscopy (DOAS) instrument and contains the NO<sub>3</sub> data [Smith, *et al.*, this issue]. In the third paper, calculations of OH and NO<sub>3</sub> using a three-dimensional (3-D) model are presented which consider the location of the island in the eastern Atlantic [T. Berntsen *et al.*, A 3-D global simulation of OH and NO<sub>3</sub>: A comparison with measurements and implications for global oxidation rates, submitted to *Journal of Geophysical Research*, 1996].

## 2. Meteorological and Air Chemical Situation at Izaña

The Izaña Instituto Nacional de Meteorología (INM) observatory is located on the Island of Tenerife, 400 km west of Africa (28°18'N, 16°30'W) in the Atlantic Ocean in the NE tradewinds region. It is meteorologically separated from Europe under most conditions, and only during a few episodes can the impact of European emissions be seen. The observatory is situated on a mountain platform at an altitude of 2370 m above sea level (asl). It is installed in the building of the INM observatory, which also contains the BAPMoN/ Global Atmospheric Watch (GAW)-station Izaña and Tropospheric Ozone Research (TOR)-station 17. The Instituto de Astrofísica de Canarias (IAC) astrophysical observatory is located approximately 1 km southwest of the INM observatory, on the same slope of the mountain. The vegetation surrounding the station is sparse. The ground is loosely covered with light volcanic material. Between 1200 m and approximately 2000 m asl., a pine forest covers most of the island.

Figure 1 shows a map of Tenerife Island with the locations of the two Izaña stations. The road, which leads to the meteorological observatory, the nearby television station, and a military camp, is closed to public traffic. Approximately 10 to 20 cars (of employees) per day pass the observatory. Also indicated is the location of the tourist road which passes the stations about 100 m downhill at a distance of 200 - 400 m. Air parcels caused by the traffic can influence the basic air chemical conditions. One such event, a strong emission of NO, was registered, which is

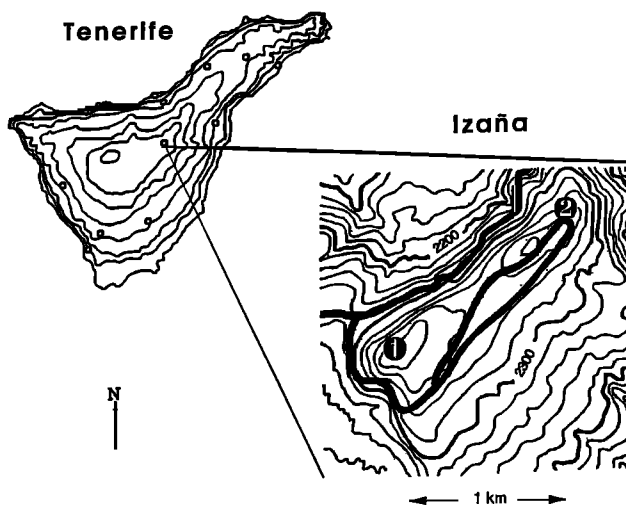


**Figure 1.** Map of Tenerife showing the location of the IAC (point 1) and of the INM (point 2) at the Izaña Plateau. Thick line marks the roads.

reflected in the OH data, thus proving the fast chemistry in which OH is involved.

The mean pressure at the station is 770 hPa. The annual mean temperature at Izaña is 9.4°C, and the precipitation is 480 mm/yr with approximately 40 precipitation days per year. Owing to the generally strong solar insolation during daytime, a local upslope windsystem superimposes the synoptic flow pattern above the inversion. Two marked valleys in the east and northwest channel the air flow. The main wind direction at the station is northwest (Figure 2) caused by the orographic structure of the valley in the northwest. This upslope windsystem is normally not present during the night. During daytime, the local wind system transports air from lower altitudes to the station. Although these air masses, in general, do not arise from the polluted boundary layer of the island, but from altitudes above the inversion, the result is a much larger variability and, normally, lower concentrations of ozone and CO<sub>2</sub> during daytime. In contrast to this, humidity and the concentrations of NO, NO<sub>2</sub>, NO<sub>3</sub>, peroxyacetyl nitrate (PAN), and nonmethane hydrocarbons (NMHC) are markedly higher during upslope conditions. The specific sources for the higher NO<sub>x</sub> and PAN concentrations during daytime are not yet known.

A predominant attribute of the area of the Canary Islands is the presence of a subsidence inversion below the elevation of the station. This inversion separates the air of the maritime boundary layer (and the polluted air from the settlements of the Island (~300,000 inhabitants) from the clean air aloft. The inversion is present approximately 90% of the time in summer and 70% in winter. In summer the upper boundary of the inversion layer lies at ~1500 m, i.e., significantly below the altitude of the station. The situation during the OH campaign May 19, 1994 is characterized in Figure 3.

Nighttime concentrations of O<sub>3</sub> under stable weather conditions, averaged over two successive nights, mostly compare well with the ozone concentration of the daytime free troposphere as measured by ozonesondes from Santa Cruz (OCTA 95) [Volz-Thomas *et al.*, 1995]. They do show correlations of high values of O<sub>3</sub> and extremely low humidities. It can be estimated from average vertical gradients that air measured during daytime is transported up to the altitude of the station from a level which is some hundred meters below the station. At lower Sun elevations

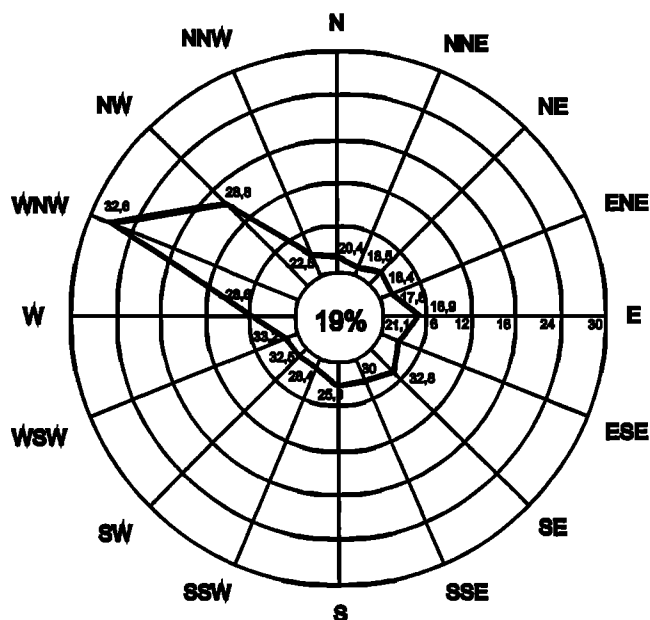


**Figure 2.** Relative frequency distribution of wind direction (mean 1961-1990, data from INM). Numbers indicate average velocities in km/h.

the influence of the orography becomes smaller. Most of the time there are almost no local influences observed between sunset and sunrise. Consequently, the variations of all trace gas concentrations are small during the night, when local influences diminish. Ozone and  $\text{CO}_2$  generally increase, humidity and anthropogenic species like  $\text{NO}/\text{NO}_2$  and  $\text{CO}$  decrease. Thus the time series of ozone and humidity show a short-term anticorrelation due to the local flow pattern. In that case, varying layers of the atmosphere are measured. During night, under conditions of free tropospheric measurements, ozone and water vapor usually also show an anticorrelation. This, however, is caused by the changing synoptic pattern when air masses of different origin and travel path reach the station. Air from the upper troposphere under conditions of transport from north show low humidities and high ozone concentrations. In contrast, air from lower altitudes or lower latitudes is often characterized by lower ozone and higher water vapor. There are exceptions when the air masses come from the Sahara, showing low ozone and low humidity too. We undoubtedly can discriminate local influences from free tropospheric air.

### 3. Instrumentation

#### MOAS Instrument

As mentioned above, a campaign which is aimed at testing the troposphere's oxidizing capacity requires the measurements of the OH and  $\text{NO}_3$  radicals. The discussion of the last two decades has shown that in situ measurements of free radicals, in particular of OH, are extremely difficult [Crosley, 1994]. A comprehensive summary on existing methods on tropospheric OH monitoring has recently been published [Crosley, 1995]. OH measurements require a sensitivity in the sub-pptv region, a considerable number of simultaneous ancillary measurements have to be made, and all measurements need a high local and temporal resolution in order to avoid averaging problems. As reported in several

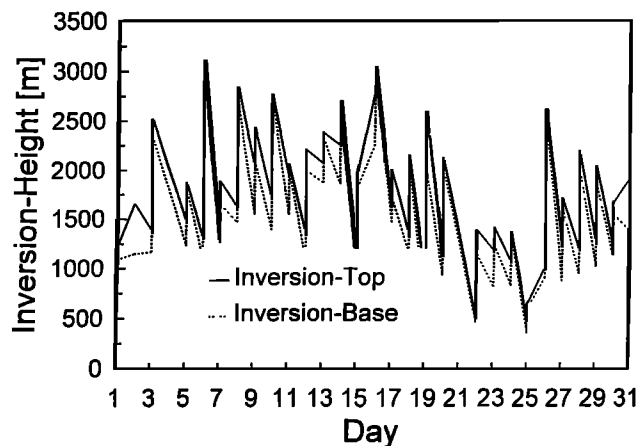


**Figure 3.** Top and base height of the inversion layer at 1200 GMT during May-19, 1994.

publications [Armerding *et al.*, 1994, 1995], the Frankfurt MOAS system meets these requirements sufficiently well.

The MOAS technique is based on absorption spectroscopy. Suitable for monitoring OH by direct absorption measurements is a spectral region in the UV at 308 nm. This interval contains some strong and well-resolved rotational lines characteristic for OH. We use the  $Q_1(2)$  line of the (0-0) band of the ( $A^2\Sigma \leftarrow X^2P$ ) transition at 307.9951 nm (vacuum line), which is one of the strongest lines, its weaker satellite, the  $Q_{21}(2)$  line at 308.0006 nm, and the  $R_2(2)$  line at 308.0231 nm. These spectral characteristics provide an unequivocal identification of the OH radical, and measurements performed in this spectral interval offer in addition a sensitive determination of  $\text{SO}_2$ ,  $\text{CH}_2\text{O}$ , and naphthalene simultaneously to that of OH.

The three main parts of the MOAS instrument are the laser spectrometer, the multipass absorption cell, and the detection unit. A schematic view is given in Figure 4. As the instrument has been described elsewhere [Armerding *et al.*, 1996] the principal parts and their function will only be discussed briefly.

The light source of the spectrometer is a rapidly tuned and (intracavity) frequency doubled cw dye ring laser (Coherent Cr 699) pumped by an 8 W argon ion laser (Coherent 318) in the all line mode. A dye mixture of Rhodamin 590, Rhodamin 610 and Kition Red S (3:3:1) is used. The cooling system of the laser is a closed recycling system.

Our procedure for rapid laser tuning is based on mode selection utilizing an angle tuned intracavity etalon. It provides a sufficiently high scanning speed and wide tuning range. In this arrangement a thin etalon (0.5 mm) with low reflectivity (20%) is mounted on a galvanometer drive. A spectral range up to  $13 \text{ cm}^{-1}$  in the UV is scanned in 100 ms. The scans are taken with a repetition rate of 1.3 kHz.

The UV generation is performed by intracavity frequency doubling using a BBO crystal positioned inside a beam waist. The bandwidth of the laser system in the UV is 7 GHz in the fast scanning mode. It is determined by the actual adjustment. The maximum cw output power is about 20 mW at 308 nm. For tropospheric OH measurements the UV intensity is reduced to 1 mW or less in order to avoid problems with laser-generated OH.

The (unavoidable) modulation of the laser radiation, caused by the spectral transmission characteristics of laser components as the Lyot filter, is highly reduced due to the stabilization and normalization of the output power using a closed-loop electrooptical modulator system. The realtime demodulation of

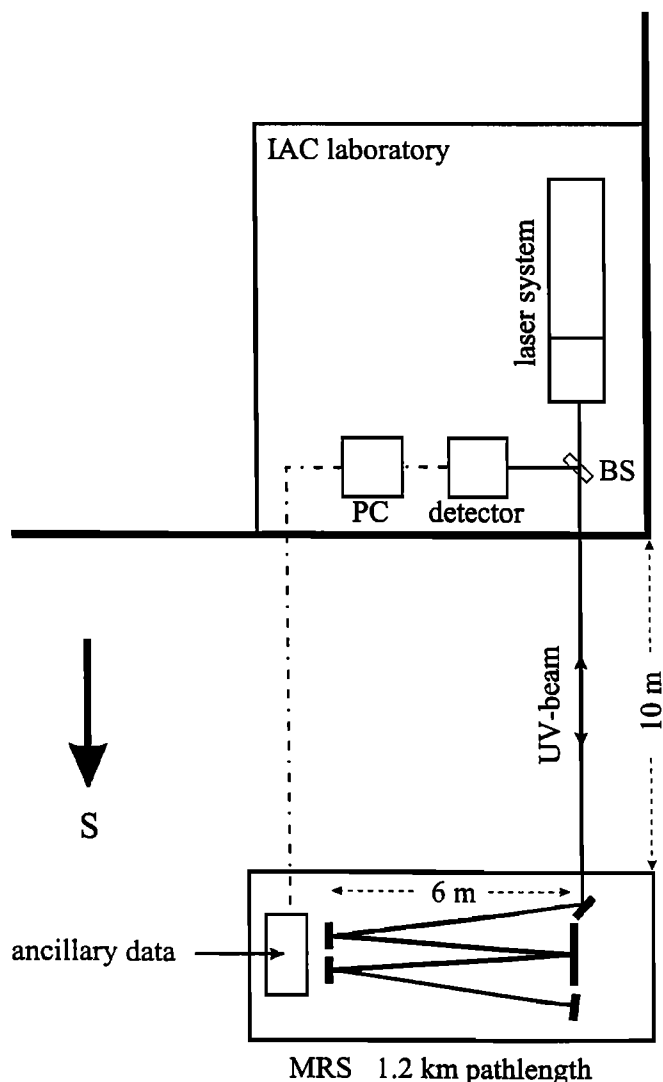


**Figure 4.** Schematic view of the MOAS instrument positioned at the IAC

the outgoing signal results in a flatness of the baseline of the order of some  $10^{-4}$ . The overall signal to noise ratio of the stabilized system is about  $8 \times 10^{-4}$  for a single line scan. The detection limit for OH is  $3\text{--}5 \times 10^5$  parts per  $\text{cm}^3$  [Armerding *et al.*, 1994, 1995, 1996] and the standard deviation for the presented measurements is smaller than  $5 \times 10^5$  OH per  $\text{cm}^3$ . In order to compensate for potential spectral jitter or drift, the system is spectrally locked using an OH spectrum taken from a flame. The OH measurements are taken as an average of 40,000 scans with an integration time of 1 min. Normally 20 - 30 measurements per hour are taken, but 60 measurements per hour are possible without direct data evaluation following.

The absorption path is folded inside a Whitecell-type multiple reflection system with a special design for tropospheric insitu measurements. The mirror system is uncovered and positioned outdoors in ambient air. It has a length of 6 m and a diameter of 0.3 m. The absorption path length is 1.2 km. The stability of the beam geometry under turbulent atmospheric conditions is assured by a reinjection technique. In this technique the laser beam at the exit of the Whitecell is inverted so as to retrace its path through the mirror system. The return beam is then separated by a beam

splitter (50%) from that entering the Whitecell. This procedure results in two advantages compared to other multipass reflection system (MRS) designs: the path length is doubled (utilizing the same mirror setup), and motions of the beam axis due to atmospheric turbulence are considerably reduced.

In the reported experimental setup a photomultiplier (Hamamatsu, R760) is utilized as the photodetector. The data acquisition is performed by a 12-bit averager having a sampling rate up to a maximum of 20 MHz (Canberra-Packard).

#### Setup of the Campaign

The supporting measurements necessary to characterize the atmospheric chemistry controlling OH include the determination of such components which quantitatively contribute to the formation and the depletion of the OH radicals as well as the determination of the different photolysis frequencies. In particular, the measurement of observables as  $J(\text{O}_3)$ ,  $J(\text{NO}_2)$ ,  $\text{O}_3$ ,  $\text{NO}_x$ ,  $\text{CH}_4$ ,  $\text{CO}$ ,  $\text{H}_2\text{O}$ , PAN, and several NMHCs are pivotal. Besides these data, information on relevant meteorological data is necessary. Temperature and pressure, for example, have an influence on reaction rates, and the orographic situation strongly determines atmospheric transport. This latter information is a critical part in model calculations. During the Izaña campaign, OH and a great number of the required ancillary data were taken by the different groups working together, and an extended data set with a data coverage for quite a number of days was obtained. Table 1 summarizes the setup of the campaign.

Since the water and power requirements of both the MOAS and the DOAS instruments could not be fulfilled simultaneously at the meteorological station, the OH measurements have been performed on the grounds of the Instituto Astrofísica de Canarias (IAC) sun observatories. OH ancillary data were recorded at both sites, one part at the IAC and the other at the INM, and several synchronously at both sites. Problems occurring from the spatial separation of the different supporting measurements were not observed. There is strong evidence for the correlation of the  $\text{O}_3$  concentration and of the water vapor recorded during the complete campaign at both sites, the IAC and the INM (Figure 5). Linear regressions of the data indicate high correlation with a slope of 0.95 and 1.1 for  $\text{O}_3$  and  $\text{H}_2\text{O}$ , respectively, and as  $R$  value of 0.97 for both.

The light source of the MOAS instrument was set up in a ground-floor laboratory of the IAC sun observatory, and the open-path multiple-reflection cell (MRS) was located in the direction south of the observatory building in a distance of about 10 m (see Figure 4). In order to align or realign the laser beam within the cell, the MRS was covered by a tent. Because of a potential influence from the tent on the experiments of the astronomers at the station, we could not begin the OH observations before late morning. Therefore OH measurements were mostly carried out between 1130 and 1630 home LT.

The ancillary data recorded directly inside the MRS include the concentration of trace components such as  $\text{O}_3$ ,  $\text{NO}$ ,  $\text{NO}_2$ , water vapor,  $\text{C}_{10}\text{H}_8$  (naphthalene),  $\text{SO}_2$ , and some data on NMHC. The NMHC samples were taken with vacuum bottles and analyzed later on at the TOR station using a gas chromatograph (GC). Also the solar radiation was determined, and the meteorological data of wind field, pressure, and temperature were continuously registered. The  $\text{NO}_x$  measurements were performed by a chemoluminescence instrument with photolysis converter (TECAN CCD 770 AL pptv) positioned inside the laboratory. The TECAN instrument

**Table 1** Instrumentation of the 1994 Tenerife Campaign Covering the Daytime Chemistry

Observable	Type of Instrument	Manufacturer	Detection Limit	Uncertainty	Temporal Resolution min.	Location
OH	MOAS	Frankfurt group		$1 \times 10^{-5}$ abs.	1	IAC
SO <sub>2</sub>	MOAS	Frankfurt group		$1 \times 10^{-5}$ abs.	1	IAC
CH <sub>2</sub> O	MOAS	Frankfurt group		$1 \times 10^{-5}$ abs.	1	IAC
C <sub>10</sub> H <sub>8</sub>	MOAS	Frankfurt group		$1 \times 10^{-5}$ abs.	1	IAC
NO <sub>2</sub>	MOAS	Frankfurt group		$1 \times 10^{-5}$ abs.	1	IAC
O <sub>3</sub>	UV-absorption	Horiba. APOA 350 E	1 ppbv	2%	1	IAC and INM
H <sub>2</sub> O	capacity	Digitron R 500		10%	1	IAC and INM
CO	GC	Trace Analytics		10%	30	INM
CH <sub>4</sub>	GC			10%	30	INM
NO	chemoluminescence		20 pptv	--	1	IAC
NO <sub>2</sub>	chemoluminescence		40 pptv	--	1	IAC
PAN	GC	Schmitt Met. Consult	1 pptv			INM
NMHCs (C2- C6)	GC	Siemens Sichromat		10%	90	INM and IAC
J(NO <sub>2</sub> )	photo-electric			20%		IAC
J(O <sub>3</sub> )	photospectrometer (cosine detector)	Brewer		20%	20	INM and IAC
	theoretical calculations					
Temperature	semiconductor			2%	1	INM and IAC
Pressure	Capacity			2%	1	INM and IAC
Wind direction				2%	1	INM and IAC
Wind direction				2%	1	INM and IAC

MOAS, multipass absorption spectrometer; IAC, Instituto de Astrofísica de Canarias; INM, Instituto de Nacional de Meteorología; GC, gas chromatography.

was coupled directly to the air mass inside the MRS via a teflon flow system. The NO<sub>x</sub> instrument was calibrated every 2 days against a calibration gas. The NO<sub>x</sub> instrument was available at the MOAS MRS for almost the entire campaign (May 11 - 25)

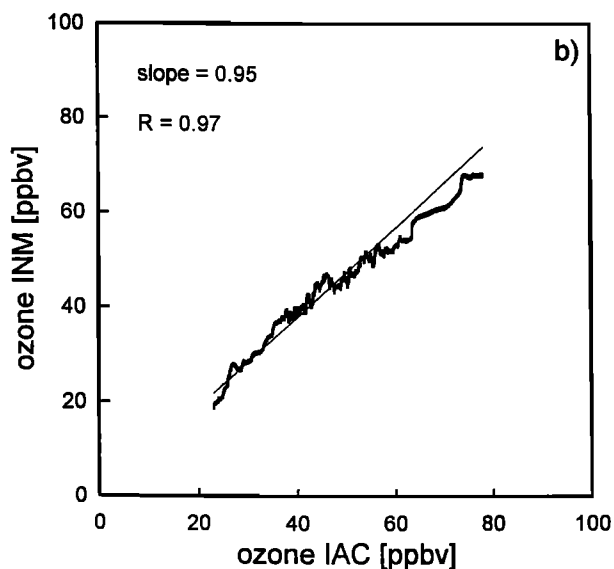
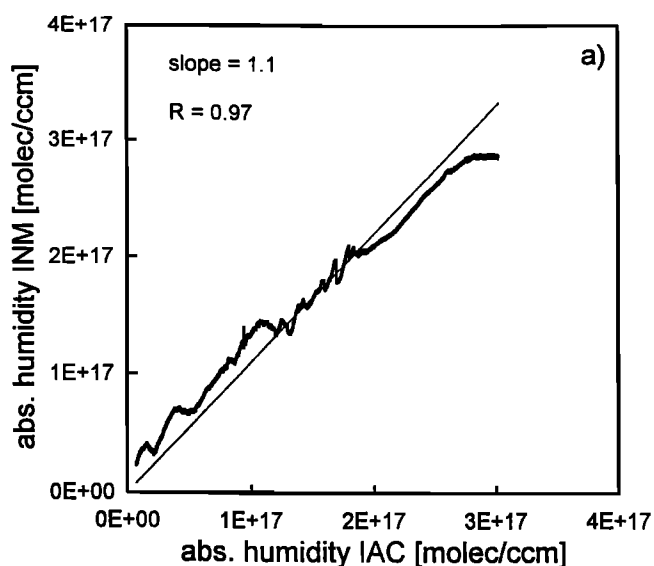
The supporting measurements at the Izaña INM meteorological observatory performed by the INM were obtained within a regular program on surface ozone, CH<sub>4</sub>, and meteorological parameters, including the vertical profile of the humidity at the Izaña GAW station. The continuous CH<sub>4</sub> measurements are properly calibrated against UFA and Natural Institute of Standards and Technology (NIST) standards. The continuous surface ozone data are calibrated with the INM, internal standard DASIBI, which has been calibrated in CMDL/NOAA laboratory. In addition, J(O<sub>3</sub>) values were obtained by calculations using global and direct UV-B measurements (290-325 nm, 0.5 nm step). The UV-B measurements were carried out daily on a routine basis with a BREWER spectrophotometer. The approximately 20-min scans are calibrated against external lamps provided by AES (Canada). The error for the UV-B data is about 8% (including the calibration). These UV-B data were completed by the time-resolved data of the measurements of a 2π global radiation detector taken at the site of the MOAS instrument. Meteorological parameters such as temperature, humidity, pressure, speed and wind direction, weather maps, situation of the inversion layer (two meteorological soundings per day) were also provided at the meteorological station. Further data of NO, NO<sub>2</sub>, NO<sub>y</sub>, PAN, NMHC (C2 - C6), and CO, CFC, O<sub>3</sub> and a third set of meteorological components were available from the TOR experiment which delivered, in particular, the TECAN instrument for the NO<sub>x</sub> measurements and three GC systems (Siemens Sichromat 2-8 for the measurements of NMHCs, trace analytical for CO, and the third system developed by R.Schmitt/Meteorologie Consult for PAN).

#### 4. Results and Discussion

As mentioned above, the Izaña station, often being under conditions of the free troposphere and, for the most part, clean tropospheric conditions, offers situations which are very favorable for the study of meteorological and chemical influences on the chemistry of the atmosphere. The chemistry of a clean environment is not as complicated, and influences from disturbances such as increased mixing ratios from pollution events and their effects on the OH concentration can be better seen, even if they are small. The hydroxyl radical is very suitable for such investigations because it reacts with many of the trace components and it has a fast response due to its high reactivity. As a result, one should expect to see these influences fairly clearly from the measurements by correlating the measured OH concentrations with these critical parameters. This should be particularly effective if, as is the case at Izaña, in addition, meteorological conditions lead to further correlations or anticorrelations.

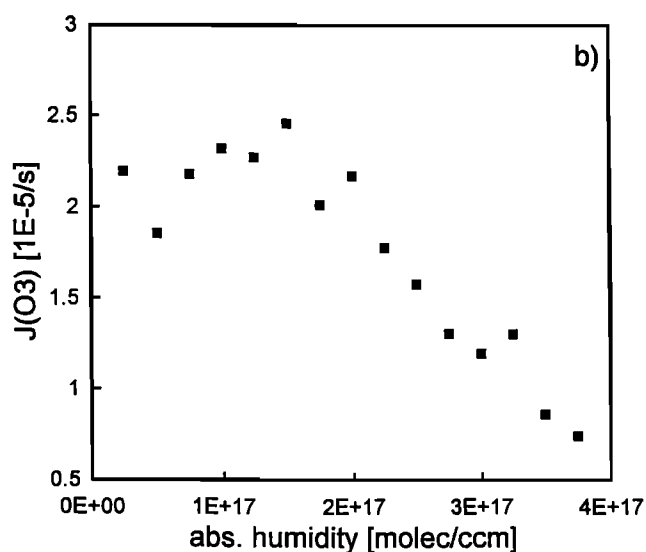
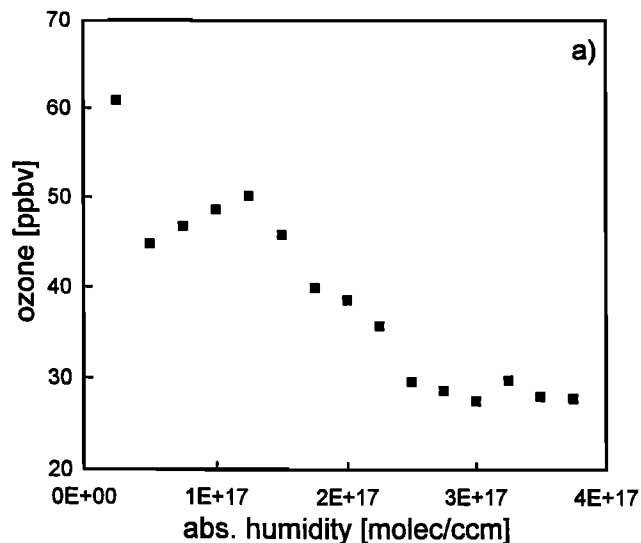
Days on which OH observations could be made were May, 11-13, 16, and 18-25. NO<sub>x</sub> data are missing for May, 13, 16, and 18. A detailed analysis of the isentropic trajectories shows that most of the air masses during the OH campaign in May 1994 came from the North Atlantic, a large percentage (about 58%) having their origin higher than 4000 m, and a few (7%) could be considered "low trajectories" starting at height levels lower than 1500 m. The analysis of isentropic parameters shows that the influence of the European and African continents is negligible during this month and that most of the air masses originate in the central or western North Atlantic at midlatitudes. This will, of course, have an influence on the observed air mass composition, since these air masses are relatively free of direct influences from anthropogenic or biogenic emissions.

In order to demonstrate effects which have the strongest



**Figure 5.** Correlations of (a) water and (b)  $O_3$ , both measured continually and simultaneously during the complete campaign at the IAC and the INM. Temporal resolution for all measurements is 1 min.

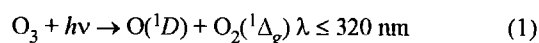
influence on the observed OH data we will in the following discuss the measurements in a more statistical way and not show the individual diurnal variations in comparison to calculations, which allows us to better follow the different trends. A discussion of the measurements with calculations of a box model will be the subject of forthcoming papers. There is, first, an interesting finding already commented on in section 2, as Figure 6a shows, namely a distinct anticorrelation of water vapor with ozone. For most of the time period of the campaign,  $H_2O$  varied only slightly over the day but often strongly from day to day. The variations in  $O_3$  were much smaller, affecting its concentration by not more than 30%. Another anticorrelation was found between  $J(O_3)$  and  $H_2O$  for quite a number of days (Figure 6b). This can possibly be explained by the upward motion of the inversion layer with increased humidity during the day combined with the fact that for most of the time during the campaign observations were made between 1130 and 1630 hours a time period in which  $J(O_3)$  decreases from its maximum value at noon.



**Figure 6.** Correlations of the absolute humidity and (a)  $O_3$  and (b)  $J(O_3)$ , taken during the entire campaign. Time resolution for  $J(O_3)$  is 20 min.

A general finding from the OH determinations is the fact that the measured OH shows fairly strong variations of its concentration over the period of observation. Figure 7 (May 22, 1994) is an example which is typical for the campaign. Not only can high OH concentrations be found, but sometimes the OH concentration is very low even in the middle of the day under optimal UV conditions. This already demonstrates the strong influence of chemical perturbations. In many cases the corresponding  $NO_x$  data also show remarkable variations with  $NO/NO_2$  ratios, being quite often as large as 1, far from photochemical equilibrium. This not only proves that the  $NO_x$  influence on OH is strong, but also that  $NO_x$  sources are not far away.

OH chemistry starts with OH production. It is well established that the primary production of the tropospheric OH radical is initiated by the UV photolysis of ozone:



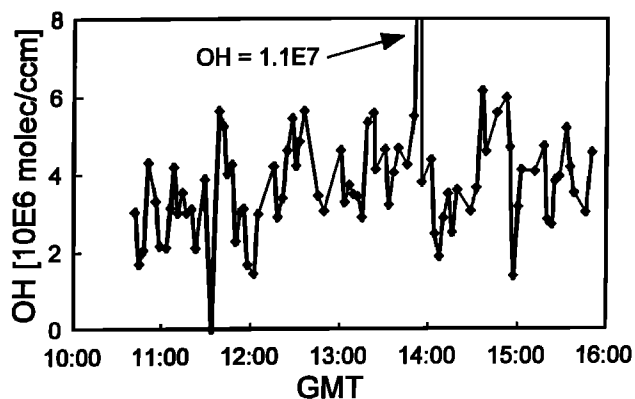


**Figure 7.** Diurnal variation of the OH concentration on May 22, 1994.

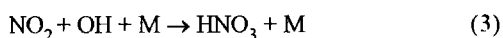
The  $O(^1D)$  formed reacts with the ubiquitous water from which two OH radicals result.



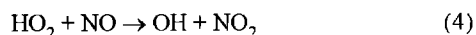
The primary OH production is therefore dependent on the product of the concentration of  $H_2O$  and the ozone photolysis rate  $J(O_3)[O_3]$ . If the primary production is a dominant factor, then this product should show a clear correlation with the measured OH. The two anticorrelations, described above, cause a damping effect on that product, which determines the primary formation of OH by ozone photolysis and reaction of the  $O(^1D)$  with water vapor. For the time period of the campaign the strongest variations in the OH primary production are therefore in the low  $H_2O$  concentration region, where the other factor, the ozone photolysis rate, is rather ineffective.

The reformation of OH by the catalytic reaction cycle propagated through reactions of peroxy radicals with NO is a further important mechanism which influences the OH concentration. For this reason, the measured NO should show a clear correlation with the observed OH. Such correlations, as discussed above, can therefore be a powerful instrument to demonstrate important sources and sinks in the OH chemistry.

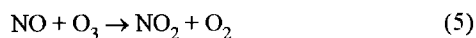
There are two effects which further favor OH recycling in its contribution to the OH concentration. The  $NO_2$  concentrations were often nearly equal to the NO concentrations, which give the OH- $NO_2$  reaction.



as a sink term for OH comparatively weaker; on the other hand, low  $O_3$  concentrations favor the OH recycling,



due to the decreasing competition with  $O_3$  in its reaction with NO:



Both effects result in higher OH concentrations.

Consumption reactions of OH are another factor influencing the observed OH concentration. Among the reactants, carbon monoxide and methane play, in general, the major role in remote areas. However, in some cases, nonmethane hydrocarbons, some

of them undergoing fast reactions with OH (e.g., isoprene), have to be considered.

With the data on  $J(O_3)$ , water vapor, and the ozone concentration, we can set up a correlation which compares the observed OH with the primary OH production. For this we need to know the influence the consumption reactions have on the OH concentration. We will start by assuming that in first approximation the OH concentration can be described by a stationary model from which OH is given by the ratio of the production term ( $P$ ) divided by the consumption term ( $C$ ) [Weinstock et al., 1980].

$$[OH]_{st} = P / C \quad (6)$$

Production processes are the primary production initiated by photolysis and the secondary production propagated through the recycling mechanism. Consumption processes are the reactions of OH with CO and  $CH_4$ . This is, of course, a simplification of the overall mechanism, but it is certainly accurate enough to discuss the main influences on the correlation diagram.  $C$  is calculated on the basis of the average concentrations of CO and  $CH_4$ , being 100 ppbv and 1.75 ppmv, respectively.

If the consumption term remains constant and the recycling mechanism is weak, then there is a direct proportionality between the rate of OH formation,  $v[OH]$ , and the production term:

$$v[OH] \sim 2 J(O_3)[O_3]k_1[H_2O] / \{k_1[H_2O] + k_2[N_2] + k_3[O_2]\} \quad (7)$$

with  $k_1$ ,  $k_2$ , and  $k_3$  the rate constants for the interaction of  $O(^1D)$  with  $H_2O$ ,  $N_2$ , and  $O_2$  [DeMoore et al., 1988]. In Figure 8a the values of this expression formed from measured values of the different factors divided by the fixed consumption term  $C$  are arranged in order of increasing OH values at which they were measured. The vertical axis is arranged in bins of  $5 \times 10^5$  OH  $cm^3$  each, according to the precision of the MOAS instrument and are ordered for increasing OH. The horizontal axis contains the number of OH  $cm^{-3}$  formed in the primary production process. All measurements of the parameters forming expression (7) and correlating with those OH concentrations which fall into such a bin are averaged and are represented by one data point. This causes a suppression of most of the strong fluctuations and helps to better work out the trends. The averaging of data is not made in this case for neighboring values on the time axis as usual, but for neighboring values on an axis which is determined by the product of the investigated chemistry, the OH. One can expect that these data are related more to each other than those on the time axis.

The diagram in Figure 8b shows the total number of single OH measurements which belong to the respective sectors of the OH abscissa, which gives us the weight of each data point on the OH axis. We can see from Figure 8b that nearly 1000 single measurements are used and that the bulk of the data is between 2 and  $5 \times 10^6$  OH  $cm^{-3}$ . OH concentrations above  $1 \times 10^7$   $cm^{-3}$  are rather scarce but do exist. For this reason, the diagrams will necessarily show some scatter for these large ordinate values, which reflects the variations of the single measurements.

It is obvious that the correlation in Figure 8a will not give a complete picture of the atmospheric chemistry at the chosen site but only describe the situation at the site for the chosen time period. OH measurements were made on 12 days, and the daily variation was measured in most cases between 1130 and 1630 hours at every day, as mentioned above. During this time period,  $J(O_3)$  did not vary much except for the presence of clouds, which was rare. The measurements at zero  $J(O_3)$ , on the other hand,

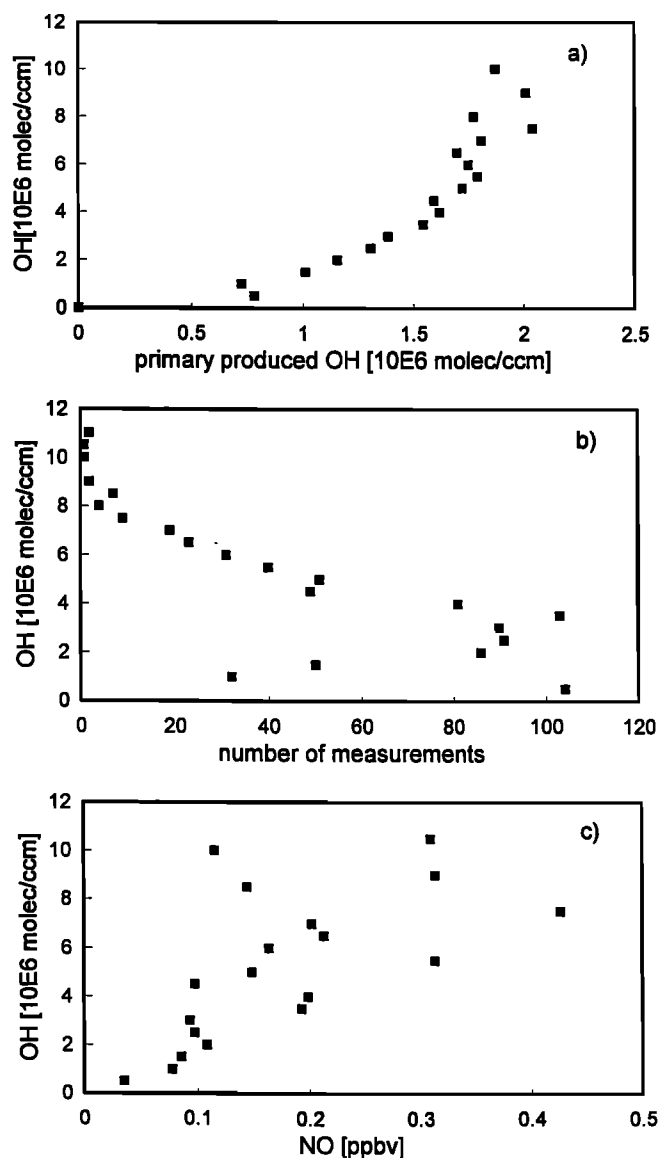


**Figure 8.** (a) Correlations of OH (measured) and primary produced OH, (b) number of single OH measurements per OH concentration interval, and (c) NO. Data are grouped into bins of  $5 \times 10^5$  OH.

were part of a regular control over the day. For this reason, the light path is shadowed by a tent, which results in zero  $J(O_3)$  and in an OH signal being below the detection limit.

We now consider recycling by the NO reactions. These reactions convert  $HO_2$  radicals, which are a product of the OH consumption reactions, back into OH, leading to an increase in the OH concentration. This increase in OH formation is dependent on the NO concentration. The measured OH concentration on the ordinate in Figure 8a shows that the additional production strongly increases nonlinearly, pointing to the influence of recycling. This same effect could also be caused by a decreasing influence of the consumption reactions. To demonstrate the importance of the recycling mechanism on the observed OH concentration we correlate the measured NO concentration with the OH values in the same way as was done for the primary production (Figure 8c). We see from the figure that OH is strongly correlated with NO. The lowest OH concentration values appear together with the lowest NO values,

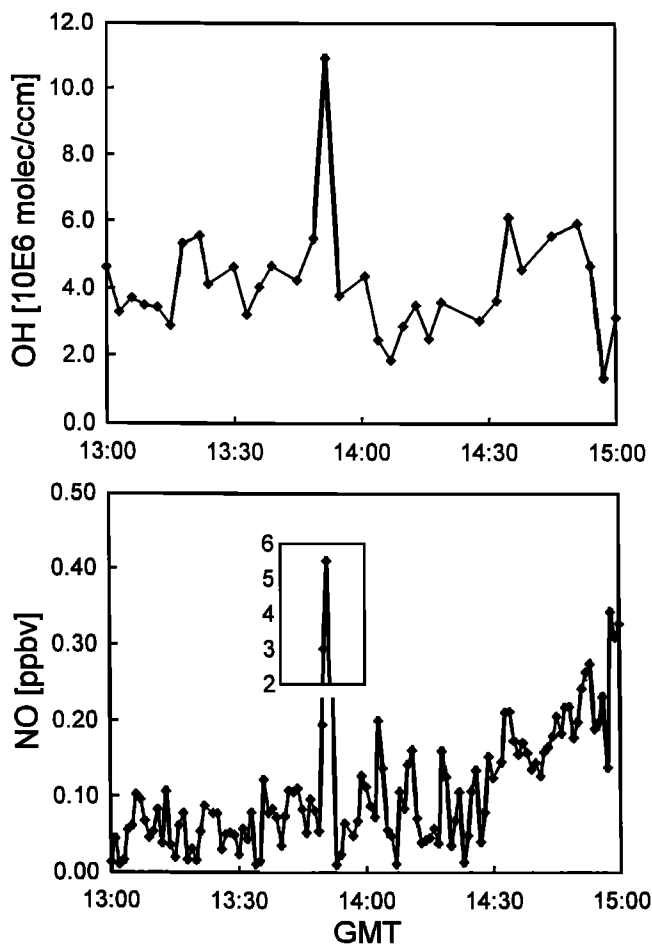


**Figure 9.** Variation of OH and NO concentrations at May 22, 1994 (car emission at 1350 hours).

and vice versa. Looking, on the other hand, at the  $CH_4$  and CO data, we see that the two components have average values of 1.75 ppmv and 100 ppbv with variations generally not larger than 2–3% and 10–15%, respectively. Under the assumption that nonmethane hydrocarbons do not contribute significant losses, the distinct curvature in Figure 8a strongly points to NO catalytic reactions, with the result that the low values of  $NO_x$  found at Tenerife favor OH production

The strong influence of NO on the OH data can also be demonstrated from a special event when a small car came near the MOAS instrument. The NO concentration raised substantially from a low value of 60 pptv to the very high value of 55 ppbv (Figure 9). The response of the OH is immediate, showing a high value at  $1.1 \times 10^7 \text{ cm}^{-3}$ . The high NO concentration accelerates the OH reformation strongly. The TECAN instrument had a repetition rate of 40 s, which means every 20 s either NO or  $NO_2$  was measured for 10 s each. The corresponding OH integration time was 60 s. This difference in the measuring cycles of the two instruments makes it difficult to quantitatively compare measured and calculated OH concentrations for this case, but the example nicely demonstrates the strong influence of NO on OH.

Carbon monoxide and methane are important reactants of the OH radical. However changes in the methane and carbon monoxide concentrations were marginal. Among the nonmethane hydrocarbons, formaldehyde is simultaneously measured with OH and extracted from the same absorption spectrum. In the OH concentration interval between  $2$  and  $8 \times 10^6 \text{ cm}^{-3}$  it increases by nearly a factor of 3, with an average value of 1 ppbv.



Measurements of other nonmethane hydrocarbons (ethane, ethene, acetylene, propane, propene, n-butane, i-butane, n-pentane, i-pentane, isoprene, n-hexane, benzene, and toluene) were made during the week before and for a few days during the first week of the campaign. Among these compounds, isoprene showed maximum values of approximately 90 pptv around noon. This made its contribution to OH depletion at least a factor of 10 larger than that from any of the other measured NMHC compounds and even larger than that of the sum of the others. Mixing ratios of about 90 pptv could be observed for several days during that period. If we assume that concentrations of a similar size were present during most of the campaign during the daytime, then its influence on the OH concentration compares with that of CO or methane. This is also valid for formaldehyde. Nonmethane hydrocarbons may therefore have a considerable effect on the OH concentration at Tenerife, which will be subject of further investigation using model calculations.

The diurnal variations of the OH concentration show fluctuations which can be rather large. Low OH concentrations near the detection limit can be found even at noon. These variations in the OH concentration are a typical result in most of the measurements. However, there are time periods when these variations are remarkably smaller. The duration of disturbances also differs greatly, ranging from the minute timescale up to an hour or more. A nice example is given in Figure 9, which shows a width that could not be resolved with time. The concentrations of  $\text{NO}_x$  were observed to vary rapidly, which may also hold for other trace gases. If these fast variations were caused by the traffic, which is very probable, then we should expect similar variations of the other emissions from automobile exhaust. The variability of biogenic emissions is unknown. Because of their high reactivity, these may also contribute to substantial short-time variations in the OH chemistry.

## 5. Conclusions

This paper describes first results from a campaign set up to test the oxidizing capacity of the troposphere, especially to study the influence of European emissions on a clean tropospheric environment. The measurements were performed at an elevation of nearly 2400 m above sea-level at the island of Tenerife. OH and  $\text{NO}_3$  measurements were carried out during the campaign to test both daytime and nighttime chemistry. OH measurements which are discussed in this paper were taken between May 11 and 25, 1994. For this time period the relevant parameters influencing the OH concentration were also monitored. The OH daily variations which are not explicitly discussed show strong variations over the day. The measured OH concentrations showed maximum values lying above  $1 \times 10^7 \text{ cm}^{-3}$  with a noontime average at  $4\text{--}5 \times 10^6 \text{ cm}^{-3}$  for the whole campaign. According to calculations using a global 3-D chemical transport model [T. Bernsten et al., submitted manuscript, 1996] the OH daily maximum is at  $7.5 (+/- 2.0)10^6 \text{ cm}^{-3}$  for that period with a daily mean at  $2.0(+/-0.5)10^6 \text{ cm}^{-3}$ . This shows that the measured noontime average, which can be compared with the calculated daily maximum, is about a factor of 2 lower than the model values.

Among the observed parameters, the  $\text{NO}_x$  concentration showed fairly strong variations similar to OH.  $\text{NO}$  and  $\text{NO}_2$  were often found not to be in photochemical equilibrium, pointing to the existence of sources not too far from the station.

To demonstrate the effects which influence the observed OH concentrations, these data are correlated with those from other parameters. The correlations clearly show the strong dependence

of measured OH on the catalytic recycling process. Also a considerable influence of nonmethane hydrocarbons can be deduced from the observations. The correlation diagrams further show that ozone and water vapor are anticorrelated with each other.

**Acknowledgments** This work has been financially supported by the European Commission (grant EV5V-CT93-0321), by the DFG, and by the Fonds der Chemischen Industrie, which is gratefully acknowledged. We would like in addition to express our thanks to the Kiepenheuer Institut für Sonnenphysik, Freiburg/Tenerife (W. Schmidt), and the Instituto de Astrofísica de Canarias (F. Sanchez), Tenerife, for their support in realizing the campaign. We thank B. Kinzer for his assistance in developing the electronic equipment.

## References

- Armerding, W., M. Spiekermann, and F. J. Comes, OH multipass absorption: An absolute and in situ method for local monitoring of tropospheric hydroxyl radicals, *J. Geophys. Res.*, 99(D1), 1225, 1994.
- Armerding, W., M. Spiekermann, J. Walter, and F. J. Comes, MOAS: An absorption laser spectrometer for sensitive and local monitoring of tropospheric OH and other trace gases, *J. Atmos. Sci.*, 52(19), 3381, 1995.
- Armerding, W., M. Spiekermann, J. Walter, and F. J. Comes, MOAS: A fast scanning laser spectrometer for the in-situ determination of atmospheric trace gas components, in particular OH, *Appl. Opt.* 35 (21), 4206, 1996.
- Comes, F. J., Recycling in the Earth's atmosphere: The OH radical - Its importance for the chemistry of the atmosphere and the determination of its Concentration, *Angew. Chem.*, 33, 1816, 1994.
- Crosley, D. R., Local measurement of tropospheric HO, NASA Conference Publication 3245, 1994.
- Crosley, D.R., Measurement of  $\text{HO}_x$  radicals in the atmosphere, *J. Atmos. Sci.* 52, 3297, 1995.
- DeMoore, W. B., S. P. Sander, M. J. Molina, D. M. Golden, R. F. Hampson, M. J. Kurylo, C. J. Howard, and A. R. Ravishankara, Chemical Kinetics and Photochemical Data for Use in Stratospheric Modeling, *Evaluation Number 8*, NASA Jet Propul. Lab. Calif. Inst. of Technol., Pasadena, 1988.
- Ehhalt, D. H., H.-P. Dorn, and D. Poppe, The chemistry of the hydroxyl radical in troposphere, *Proc. R. Soc. Edinburgh*, 97B, 17-34, 1991.
- Finlayson-Pitts, B. J. and J. N. Pitts, *Atmospheric Chemistry*, pp. 961-999, John Wiley, New York, 1986a.
- Finlayson-Pitts, B. J. and J. N. Pitts, *Atmospheric Chemistry*, pp. 536-538, John Wiley, New York, 1986b.
- Smith, N., H. Coe, J.M.C. Plane and E. Cuevas, Observations of the Nitrate Radical in the free troposphere at Izaña de Tenerife, *J. Geophys. Res.*, this issue.
- Volz-Thomas, A., R. Schmitt, H. Fischer, McKenna, and M. Mihelcic, Oxidising capacity of the tropospheric atmosphere, Final report to the European Commission, Contract EV5V - CT91 - 0042, June 1995.
- Weinstock, B., H. Niki, and T. Y. Chang, Chemical factors affecting the hydroxyl radical concentration in the troposphere, *Adv. Environ. Sci. Technol.*, 10, 221-258, 1980.
- W. Armerding, F. J. Comes, H. J. Crawack, O. Forberich, G. Gold, C. Rueger, M. Spiekermann, and J. Walter, Institut fuer Physikalische und Theoretische Chemie, Johann Wolfgang Goethe-Universitaet, Marie Curie Str. 11, 60439 Frankfurt, Germany. (e-mail: comes@chemie.uni-frankfurt.de)
- E. Cuevas and A. Redondas, Izaña GAW Station, Instituto Nacional de Meteorologia, 38071 Santa Cruz de Tenerife, Islas Canarias, Spain. (e-mail: ecuevas@ull.es)
- P. Matuska and R. Schmitt, Meteorologie Consult, Auf der Platt 47, 61479 Glashuetten, Germany.

(Received February 29, 1996; revised November 17, 1996; accepted November 17, 1996.)